reomeric excess had occurred during these synthetic transformations. The SAMP hydrazone was then alkylated with ethyl iodide and subjected to basic elimination with DBN at −78 °C. The conversion of hydrazone (*S,S*)-17 to nitrile (*S*)-7 took place in only fair yield, and no attempt was made to improve this reaction. The overall yield of (*S*)-7 from (*S,S*)-13a was 25%. Although no direct measure of ee was made on (*S*)-7, it is presumed to be in the range of 70–85% based on results obtained with monomer (*S*)-4. Following silica gel chromatography (*S*)-7 was obtained in analytically pure state and had identical spectral characteristics to its racemate.

Physical Methods of Characterization. Differential scanning calorimetry (DSC) experiments were conducted with a Perkin Elmer DSC 4 differential scanning calorimeter. Typically, heating and cooling rates of 10 °C min⁻¹ were employed. Samples for DSC experiments (2–7 mg) were prepared in hermetically sealed aluminum pans. Microscopic observations were made on a Leitz Laborlux 12 pol polarizing microscope coupled to a Leitz hot stage, controlled by a Research, Inc. thermocontroller. Samples were prepared on clean glass surfaces by melting a small particle of the material on the surface at an appropriate temperature. A second glass cover slip was placed on top of the droplet, and the sample was flattened into a thin film.

Appendix

Figure 9 shows a scheme for deducing the structures of condensation macromolecules at the level of regiochemical order. Chain segments are represented as their Fisher projections where individual monomer units are assembled with a generic linking group symbolized as "–O–". The detailed structure of the linking group is not important for the following discussion. Beginning with a highly substituted, highly symmetric chain, removal of substituents in an orderly fashion will uncover the various levels of macromolecular structure. Removing a pair of substituents

from each monomer unit such that each pair is removed from *equivalent positions in adjacent monomers* leaves the *isoregic* backbone. This structure is characterized by its polar translational symmetry. Similarly, removing a pair of substituents from each monomer unit such that each pair is removed from *nonequivalent positions in adjacent monomers* leaves the *syndioregic* backbone. This structure is characterized by its apolar translational symmetry with a periodicity of two monomer units. The *aregic* backbone is obtained by randomly removing pairs of substituents from either equivalent or nonequivalent positions in adjacent monomer units. Chains of this type are not characterized by a single structure but instead by a set of possible constitutional isomers. The aregic backbone thus belongs to the family of chemically disordered polymers.

Figure 10 shows a scheme for deducing the chiral forms of condensation macromolecules. Using Figure 9 as a starting point, stereogenic elements can be introduced by further removal of the remaining substituents on each chain. It can be seen that each of the regiochemical structures can exist in configurationally ordered (top row, Figure 10) as well as configurationally disordered forms (bottom row, Figure 10). Looking first at the disordered forms, it is interesting to note that it is possible to have complete stereochemical and regiochemical order and still have an achiral backbone. The *meso isoregic* and the *meso syndioregic* structures are such examples. The meso isoregic backbone contains a glide-reflection axis along the chain direction, while the meso syndioregic possesses mirror planes perpendicular to the backbone. The configurationally disordered forms of the isoregic and syndioregic backbones as well as the configurationally disordered aregic backbone are systems best described as a set of possible diastereomeric isomers.

Claisen Rearrangement of Allyl Phenyl Ether. 1-^{14}C and β-^{14}C Kinetic Isotope Effects. A Clearer View of the Transition Structure

Lidia Kupczyk-Subotkowska,[1] **Witold Subotkowski,**[1] **William H. Saunders, Jr.,**[*,2] **and Henry J. Shine**[*,1]

Contribution from the Department of Chemistry and Biochemistry, Texas Tech University, Lubbock, Texas 79409, and Department of Chemistry, University of Rochester, River Station, Rochester, New York 14627. Received October 28, 1991

Abstract: The kinetic isotope effects, $k^{12}C/k^{14}C$, for the rearrangements of allyl [1-^{14}C]phenyl ether and [β-^{14}C]allyl phenyl ether have been measured: 1.0119 ± 0.0009 and 1.0148 ± 0.0005, respectively. These results, along with those reported earlier for ^{18}O, 2-^{14}C, α-^{14}C, and γ-^{14}C, represent the first complete kinetic isotope effect (KIE) description of a pericyclic system. Modeling calculations have been applied to the heavy-atom KIE and the previously reported deuterium KIE to define the transition structure of the rearrangement more explicitly. The calculations confirm our earlier description that the C_α–O bond is 50–60% broken while the C_γ–C_{ortho} bond is 10–20% formed and now provide significantly more insight to the dynamics of the rearrangement. Coupling between the phenoxy and allyl fragments is stronger, and within the fragments is weaker, than previously supposed.

Introduction

Recently, we reported kinetic isotope effects (KIE) for the four atoms that are directly involved in bond breaking and bond forming in the thermal rearrangement of allyl phenyl ether.[3] That

is, we measured the ^{18}O and α-^{14}C KIE of bond breaking and the *ortho*-^{14}C and γ-^{14}C of bond forming. The results were combined with α- and γ-deuterium KIE that had been reported earlier by McMichael and Korver[4] to characterize the transition structure

---

(1) Texas Tech University.
(2) University of Rochester.

(3) Kupczyk-Subotkowska, L.; Saunders, W. H., Jr.; Shine, H. J. *J. Am. Chem. Soc.* **1988**, *110*, 7153.

Scheme I
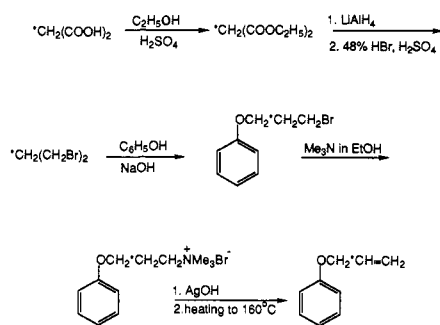
Table I. Kinetic Isotope Effects (KIE) for the Thermal Rearrangement of Allyl [1-^{14}C]Phenyl Ether and [β-^{14}C]Allyl Phenyl Ether in Diphenyl Ether at 220 °C

label	expt	conv	KIE
1-^{14}C	1	0.27	1.0115 ± 0.0017
		0.20	1.0120 ± 0.0020
		0.18	1.0106 ± 0.0008
1-^{14}C	2	0.30	1.0114 ± 0.0012
		0.23	1.0124 ± 0.0015
		0.15	1.0135 ± 0.0017
		mean	1.0119 ± 0.0009
β-^{14}C	3	0.29	1.0136 ± 0.0011
		0.25	1.0168 ± 0.0017
		0.16	1.0142 ± 0.0011
β-^{14}C	4	0.27	1.0135 ± 0.0011
		0.22	1.0149 ± 0.0011
		0.16	1.0148 ± 0.0015
		mean	1.0148 ± 0.0005

Table II. Averaged KIE for the Rearrangement of **1** into **2**

isotope	KIE	isotope	KIE
^{18}O	1.0297[a]	1-^{14}C	1.0148
α-^{14}C	1.0306[a]	2-^{14}C	1.0375[a]
β-^{14}C	1.0119	α-^{2}H$_2$	1.18[b]
γ-^{14}C	1.0362[a]	γ-^{2}H$_2$	0.95[b]

[a] Reference 3. [b] Reference 4, at 180 °C.

minor changes have been made to keep **3** and **4** consistent with **5** and **6**, but these did not significantly alter KIE calculated using the same bond couplings as before.[3]

of this well-known sigmatropic rearrangement.[3] It was found by cutoff-model calculations that the C$_\alpha$–O bond was 50–60% broken while C$_\gamma$–C$_{ortho}$ bond formation was only 10–20% complete in the transition structure. During the course of these calculations, it becomes apparent that substantial KIE should also be experienced at the C$_1$ and C$_\beta$ positions. That is, the calculations indicated that KIE for these atoms should result from coupled motion throughout the six-atom array of this pericyclic system. Therefore, we set out to measure these KIE and have substantiated the indications. Substantial 1-^{14}C and β-^{14}C KIE have been found. We report them here and use them with the earlier heavy-atom and deuterium KIE to refine our view of the transition structure of the rearrangement.

Results

Allyl [1-^{14}C]phenyl ether ([1-^{14}C]-**1**) was prepared from 4-nitro[1-^{14}C]phenol in standard ways. [β-^{14}C]Allyl phenyl ether was prepared in five steps as shown in Scheme I. The key, labeled intermediate in these steps was [2-^{14}C]-1,3-propanediol. Attempts to prepare 1,3-propanediol in good yield by direct reduction of malonic acid with LiAlH$_4$ were unsuccessful, and it was found to be expedient to reduce the diethyl ester. Standard procedures were used in all other steps.

Rearrangements of **1** into **2** were carried out at 220 °C as described earlier,[3] and the isolated **2** was converted into its phenylurethane for purification by sublimation and scintillation counting. The KIE are listed in detail in Table I and are summarized with those reported earlier in Table II.
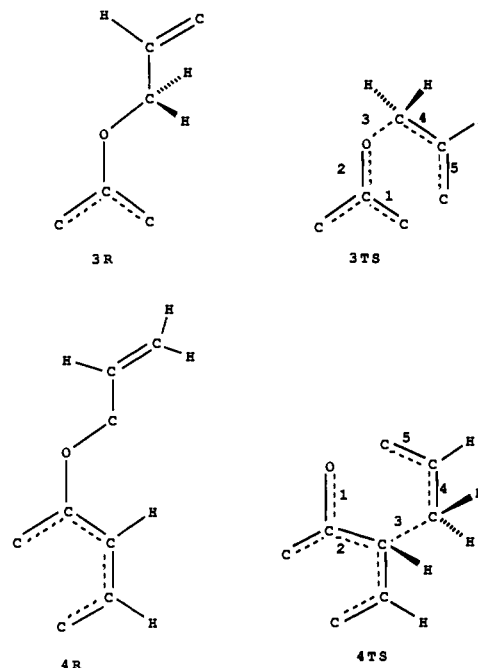
Calculations

The model calculations were carried out as before,[3] using the BEBOVIB-IV program in a version compiled to run on a Macintosh II computer.[5] The models **3R** → **3TS** and **4R** → **4TS** correspond to **5** → **6** and **7** → **8**, respectively, in the earlier work.[3] A few

When models **3** and **4** were used to calculate the β-^{14}C and 1-^{14}C effects, the resulting values were quite large: on the order of 1.03–1.04 in both cases. These models are, however, not true cutoff models[6,7] with respect to these effects, and the values are thus of uncertain reliability. Further elaboration of **3** and **4** to make them true cutoff models for all of the observed effects would require cyclic transition structures. As we have pointed out before,[3] cyclic transition structures introduce redundancies that considerably complicate the performance and interpretation of the calculations.[8] Consequently, we decided to use two additional models, **5R** → **5TS** and **6R** → **6TS** to calculate the β-^{14}C and 1-^{14}C effects.
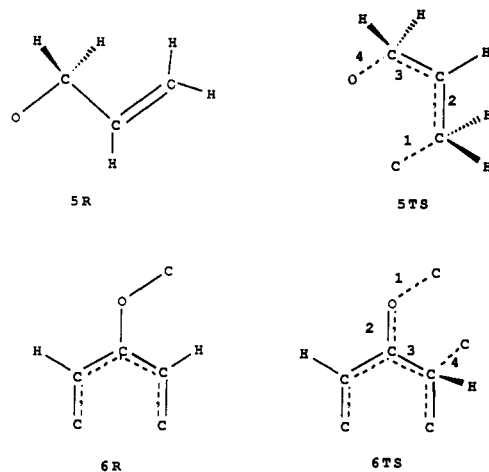
(4) McMichael, K. D.; Korver, G. L. *J. Am. Chem. Soc.* **1979**, *101*, 2746.

(5) Sims, L. B.; Burton, G. W.; Lewis, D. E. BEBOVIB-IV, QCPE No. 337; Department of Chemistry, Indiana University, Bloomington, IN. The Macintosh II version has been submitted to QCPE.

(6) Wolfsberg, M.; Stern, M. *J. Pure Appl. Chem.* **1964**, *8*, 225.

(7) Stern, M.; Wolfsberg, M. *J. Chem. Phys.* **1966**, *45*, 4105.

(8) Keller, J. H.; Yankwich, P. *J. Am. Chem. Soc.* **1974**, *96*, 2303.

Table III. Calculated Isotope Effects for Strong Coupling within Allyl and Phenoxy Fragments[a]

$n(CO)/n(CC)$	^{18}O	α-d	α-^{14}C	β-^{14}C	γ-^{14}C	γ-d	$ortho$-^{14}C	1-^{14}C	Dev(hvy)	Dev(H/D)
0.5/0.2	1.0308	1.1610	1.0338	1.0496	1.0398	0.9393	1.0377	1.0382	0.0194	0.0196
0.5/0.1	1.0308	1.1610	1.0338	1.0454	1.0461	0.9692	1.0404	1.0358	0.0178	0.0258
0.4/0.3	1.0309	1.1951	1.0367	1.0512	1.0386	0.9383	1.0384	1.0396	0.0204	0.0178
0.3/0.3	1.0309	1.2318	1.0401	1.0502	1.0428	0.9653	1.0426	1.0397	0.0206	0.0468
0.4/0.2	1.0309	1.1951	1.0367	1.0489	1.0441	0.9657	1.0422	1.0383	0.0196	0.0209
exptl	1.0297	1.18	1.0306	1.0148	1.0362	0.95	1.0375	1.0119		

[a] a_{mn} values 0.8, 0.5, 0.5, 0.8 for models **3** and **4**, 0.5, 0.8, 0.5 for models **5** and **6**. The order is that of the numbered bonds in the corresponding structures. Tunnel corrections calculated from the first term of the Bell equation are included in all isotope effects, but change the effects by less than experimental error.

Table IV. Calculated Isotope Effects for Strong Coupling between Allyl and Phenoxy Fragments[a]

$n(CO)/n(CC)$	^{18}O	α-d	α-^{14}C	β-^{14}C	γ-^{14}C	γ-d	$ortho$-^{14}C	1-^{14}C	Dev(hvy)	Dev(H/D)
0.5/0.2	1.0316	1.1654	1.0354	1.0231	1.0357	0.9391	1.0254	1.0182	0.0073	0.0169
0.5/0.1	1.0316	1.1654	1.0354	1.0199	1.0381	0.9635	1.0276	1.0164	0.0054	0.0188
0.4/0.3	1.0299	1.1980	1.0366	1.0248	1.0370	0.9412	1.0270	1.0194	0.0076	0.0178
0.3/0.3	1.0279	1.2321	1.0376	1.0242	1.0411	0.9683	1.0309	1.0195	0.0071	0.0482
0.4/0.2	1.0299	1.1980	1.0366	1.0227	1.0400	0.9658	1.0294	1.0183	0.0065	0.0226
exptl	1.0297	1.18	1.0306	1.0148	1.0362	0.95	1.0375	1.0119		

[a] a_{mn} values 0.4, 0.65, 0.65, 0.4 for models **3** and **4**, 0.75, 0.45, 0.75 for models **5** and **6**. The order is that of the numbered bonds in the corresponding structures. Tunnel corrections calculated from the first term of the Bell equation are included in all isotope effects, but change the effects by less than experimental error.

As before, off-diagonal F matrix elements were introduced to achieve an imaginary reaction coordinate frequency in which bonding changes were occurring in such a way as to transform the transition structures to products.[9] The off-diagonal elements are calculated from eq 1, and the a_{mn} values for models **3** and **4** are given by eq 2. A different relation, eq 3, is required for models

$$F_{mn} = a_{mn}(F_{mm}F_{nn})^{1/2} \qquad (1)$$

$$1 - a_{12}^2 - a_{23}^2 - a_{34}^2 - a_{45}^2 + a_{12}^2 a_{34}^2 + a_{12}^2 a_{45}^2 + a_{23}^2 a_{45}^2 = D \qquad (2)$$

$$1 - a_{12}^2 - a_{23}^2 - a_{34}^2 + a_{12}^2 a_{34}^2 = D \qquad (3)$$

5 and **6** because they contain four rather than five consecutive reacting bonds. As a result, using the same set of a_{mn} values for corresponding bond couplings in models **3** and **4** on the one hand, and **5** and **6** on the other, can lead to imaginary frequencies of quite different magnitudes.

To avoid this physically unrealistic situation, we chose a_{mn} values for our models (except those reported in Table II) as follows. Couplings within the allyl and phenoxy fragments (a_{12} and a_{45} in 3TS and 4TS, and a_{23} in 5TS and 6TS) were assigned similar but not identical values. Couplings between the fragments (a_{23} and a_{34} in 3TS and 4TS, and a_{12} and a_{34} in 5TS and 6TS) were assigned different sets of values, but again values that were similar for all between-fragment couplings. Thus, corresponding a_{mn}'s in different models (e.g., a_{34} in 3TS and 5TS or a_{23} in 4TS and a_{34} in 6TS) were not necessarily the same, but the *ratios* of a_{mn}'s for adjacent "within-fragment" and "between-fragment" couplings were kept reasonably similar (e.g., a_{12}/a_{23} in 3TS and a_{23}/a_{21} in 6TS). In this way we could allow the couplings to vary so as to give good fits to all of the experimental results, without treating as completely independent, couplings that physically are not.

Our adjustable parameters, then, are the $n(CO)$, $n(CC)$, and a_{mn} values. We began with a set of five $n(CO)$ and $n(CC)$ values that led to the best agreements with the six experimental isotope effects quoted previously.[1] The initial set of a_{mn} values were the same as those of Table VII in ref 1. The results are given in Table III.

Before discussing these results, some comment on the criteria for goodness of fit is in order. Previously, we simply compared one by one the isotope effect predictions of a given model with the corresponding experimental values and rejected the model if one or more of the predictions was off by a significant amount. This approach becomes increasingly cumbersome and subjective as the number of comparisons to be made increases. Consequently,

(9) Melander, L.; Saunders, W. H., Jr. *Reaction Rates of Isotopic Molecules*; Wiley-Interscience: New York, 1980; pp 64–66.

the last two columns of each table give deviations calculated from eq 4. The form of eq 4 is essentially the same as that of the

$$\text{Dev} = \left(\sum_{1}^{n}((\text{exptl} - \text{calcd})/\text{exptl})^2/(n-1)\right)^{1/2} \qquad (4)$$

equation used to calculate relative standard deviations (replacement of "calcd" by "mean" and "Dev" by "s_{rel}" would make them identical). The significance of Dev is, of course, different from that of s_{rel}, but its values have the advantage of being comparable in magnitude to relative standard deviations. The heavy-atom and H/D effects are treated separately because the uncertainty in the latter is much greater than in the former.

For example, an experimental uncertainty of ±0.02 in the two H/D effects is to be expected and corresponds to Dev(H/D) = 0.0270. The experimental uncertainty in the heavy-atom effects is harder to pin down. Uncertainties in individual values run 0.001–0.004 (Table I of ref 1 and Table I of the present paper). The most stringent measure of precision, the range of repeated determinations, is usually no more than 0.004–0.006, though in a few cases it is wider. An *average* deviation of 0.004 for the heavy-atom effects corresponds to Dev(hvy) = 0.0043 and a deviation of 0.005 to Dev(hvy) = 0.0053. These would seem to be reasonable values to aim for, while reserving the right to reject models where most effects are predicted very closely but one is significantly off. The squaring of (exptl − calcd) in eq 4 in fact tends to signal such a situation by exaggerating the contributions of very poor fits to the sum.

Returning to Table III, it is immediately evident that the calculated β-^{14}C and 1-^{14}C effects are much larger than the experimental ones. Our prediction of significant β-^{14}C and 1-^{14}C isotope effects is obviously born out by experiment, but models that predicted the other effects well are clearly unsatisfactory when confronted by the new data.

Our previous experience tells us that the magnitudes of the heavy-atom effects are quite sensitive to the couplings used; the larger the a_{mn} value coupling the two reacting bonds to a given atom, the larger the isotope effect from that atom. Thus, it was clear that we needed to reduce the within-fragment bond couplings in order to bring the β-^{14}C and 1-^{14}C effects closer to the experimental values. A concomitant increase in the between-fragment couplings is necessary to retain an imaginary reaction coordinate frequency (negative D in eqs 2 and 3).

As predicted, this change reduced the calculated β-^{14}C and 1-^{14}C effects to values in reasonable agreement with the experimental ones, but at the same time threw out of agreement some of the other effects. After considerable experimentation, promising results were obtained. The best values in Table IV (for $n(CO)/n(CC)$ = 0.5/0.1) show an average error in the heavy-atom

Table V. Calculated Isotope Effects for Best Model with Strong Coupling between Allyl and Phenoxy Fragments[a]

$n(CO)/n(CC)$	^{18}O	$\alpha\text{-}d$	$\alpha\text{-}^{14}C$	$\beta\text{-}^{14}C$	$\gamma\text{-}^{14}C$	$\gamma\text{-}d$	ortho-^{14}C	$1\text{-}^{14}C$	Dev(hvy)	Dev(H/D)
0.9/0.1	1.0412	1.0443	1.0261	1.0183	1.0240	0.8686	1.0144	1.0151	0.0126	0.1434
0.7/0.3	1.0382	1.1006	1.0290	1.0232	1.0258	0.8687	1.0184	1.0173	0.0110	0.1089
0.5/0.5	1.0345	1.1620	1.0321	1.0256	1.0257	0.8702	1.0208	1.0186	0.0104	0.0854
0.3/0.7	1.0299	1.2292	1.0350	1.0260	1.0254	0.8745	1.0227	1.0196	0.0101	0.0898
0.1/0.9	1.0236	1.3025	1.0369	1.0234	1.0251	0.8822	1.0243	1.0194	0.0098	0.1260
0.7/0.2	1.0382	1.1006	1.0290	1.0205	1.0291	0.8917	1.0205	1.0156	0.0093	0.0911
0.7/0.1	1.0382	1.1006	1.0290	1.0173	1.0315	0.9149	1.0218	1.0139	0.0081	0.0768
0.6/0.3	1.0365	1.1306	1.0306	1.0226	1.0296	0.8922	1.0222	1.0166	0.0087	0.0739
0.6/0.2	1.0365	1.1306	1.0306	1.0200	1.0330	0.9159	1.0243	1.0154	0.0071	0.0552
0.6/0.1	1.0365	1.1306	1.0306	1.0171	1.0354	0.9397	1.0256	1.0138	0.0061	0.0432
0.5/0.4	1.0345	1.1621	1.0321	1.0240	1.0297	0.8930	1.0236	1.0174	0.0084	0.0619
0.5/0.3	1.0345	1.1621	1.0321	1.0221	1.0335	0.9167	1.0260	1.0165	0.0067	0.0382
0.5/0.2	1.0345	1.1620	1.0321	1.0197	1.0370	0.9412	1.0281	1.0154	0.0053	0.0178
0.5/0.1	1.0345	1.1620	1.0321	1.0169	1.0394	0.9658	1.0294	1.0137	0.0045	0.0226
0.4/0.3	1.0323	1.1949	1.0336	1.0216	1.0375	0.9425	1.0299	1.0166	0.0052	0.0149
0.4/0.2	1.0323	1.1949	1.0336	1.0194	1.0410	0.9678	1.0320	1.0154	0.0044	0.0226
0.4/0.1	1.0323	1.1949	1.0336	1.0168	1.0436	0.9931	1.0332	1.0138	0.0043	0.0471
0.3/0.3	1.0299	1.2292	1.0350	1.0212	1.0417	0.9696	1.0338	1.0168	0.0050	0.0465
0.3/0.2	1.0299	1.2292	1.0350	1.0191	1.0452	0.9956	1.0359	1.0163	0.0052	0.0636
0.3/0.1	1.0299	1.2292	1.0350	1.0168	1.0478	1.0218	1.0371	1.0147	0.0056	0.0863
exptl	1.0297	1.18	1.0306	1.0148	1.0362	0.95	1.0375	1.0119		

[a] a_{mn} values 0.4, 0.72, 0.57, 0.4 for model **3**, 0.4, 0.73, 0.57, 0.4 for model **4**, 0.8, 0.4, 0.75 for model **5**, and 0.75, 0.4, 0.8 for model **6**. The order is that of the numbered bonds in the corresponding structures. Tunnel corrections calculated from the first term of the Bell equation are included in all isotope effects, but change the effects by less than experimental error.

effects of ±0.005, though the ortho-^{14}C effect is low by 0.01. Still more experimentation was required to get significantly better results—some 30 sets of a_{mn} values in all were tried.

Improvement resulted when the requirement that the a_{mn} values within a given model be symmetrically disposed about the midpoint (atom or bond) of the set of reacting bonds was dropped. This assumption was originally made only for the purpose of limiting somewhat the dauntingly wide range of possibilities. There is, however, no need to suppose that the fragments are coupled by identical off-diagonal F matrix elements at both ends. The results of the best attempt without this restriction are given in Table V.

The fits for $n(CO)/n(CC)$ = 0.5/0.1 and 0.4/0.2 are the best, reproducing the H/D effects within experimental error and the heavy-atom effects within ±0.004 of experiment. The worst fit to experiment is of the ortho-^{14}C effects: off by 0.008 for n-$(CO)/n(CC)$ = 0.5/0.1. To ensure that these really were the only good fits, the same range of $n(CO)/n(CC)$ values used previously (Table VII of ref 1) was explored. No other values gave acceptable fits. The fits of the two models above to experiment are probably not quite within experimental error, but these models seem to be the best obtainable without a very much more extensive and laborious search of parameter space. Since all of the models that approach the agreement of the two best ones have similar n-$(CO)/n(CC)$ and a_{mn} values, it is doubtful that such a search would be worthwhile.

Discussion

What insights, which were not apparent before, do these additional experimental and calculational results give us? Bond orders in the transition structures remain essentially unchanged: 50–60% rupture of the C_α–O bond and 10–20% formation of the C_γ–C_{ortho} bond. We know, however, significantly more about the *dynamics* of the process. Coupling between the phenoxy and allyl fragments is stronger, and within the fragments weaker, than we previously supposed. Reaction coordinate frequencies are of quite low magnitude (50i cm^{-1} or less), indicating only very slight curvature of the energy surface in the vicinity of the transition state. Even though tunnel corrections based on the first term of the Bell equation[10] are included in all cases, the corrections are well within the experimental uncertainty of the effects. The final picture of the transition structure that emerges is one in which the fragments are loosely bound to each other in the usual sense, but where the electron shifts between the fragments are strongly coupled. As far as we know, this is the first time in which the

total skeletal motion of a pericyclic system has been defined experimentally.

Experimental Section

Preparation of Allyl [1-^{14}C]Phenyl Ether. 4-Nitro[1-^{14}C]phenol was prepared in the usual way[11] from commercially-available [2-^{14}C]acetone that had been diluted with unlabeled acetone. The product, 57% after column chromatography (64 mCi/mol), was reduced to 4-amino[1-^{14}C]phenol, which was converted into [1-^{14}C]phenol in standard ways.[12] The phenol was converted into allyl[1-^{14}C]phenol by reaction with allyl bromide as described previously.[3] The final enrichment was 7.3 mCi/mol, and the overall yield, based on acetone, was 18%.

Preparation of [β-^{14}C]Allyl Phenyl Ether. The route to this compound is shown in Scheme I; the key intermediate was [2-^{14}C]-1,3-dibromopropane. 1,3-Propanediol was needed for the preparation of 1,3-dibromopropane. Attempts to prepare 1,3-propanediol in good yield by direct reduction of malonic acid with LiAlH₄ were unsuccesful. The better overall yield was obtained by reduction of the first-formed diethyl ester.

A 50-mL ethanol solution containing 10.4 g of malonic acid and 4 mL (1.0 mCi) of an aqueous ethanol solution of [2-^{14}C]malonic acid (ICN) was evaporated to dryness under reduced pressure. The residue was again dissolved in 50 mL of ethanol and evaporated to dryness. This procedure was repeated four times. The dry residue, now enriched at 10 mCi/mol, was boiled under reflux for 11 h in 50 mL absolute ethanol containing 1.0 mL of concentrated sulfuric acid. The ethanol was evaporated, and the product was extracted with ether. Workup and distillation under reduced pressure gave 13.0 g (0.81 mmol, 81%) of diethyl [2-^{14}C]-malonate. The diethyl malonate was converted into [2-^{14}C]-1,3-dibromopropane without isolation of the intermediate, 1,3-propanediol, by the procedure used by Bak and Led for preparing [^{13}C]-labeled dibromopropane.[13] (We practiced this procedure with unlabeled diethyl malonate and obtained a 56% yield of 1,3-dibromopropane. However, when labeled diethyl malonate was used, the yield of 1,3-dibromopropane fell to 8%, a blow that we attributed to our having used a new batch of unsuspectedly low-quality LiAlH₄. We report this as a warning note to other experimenters.) Owing to the low yield of labeled 1,3-dibromopropane, dilution was necessary for the subsequent steps, and the [2-^{14}C]-1,3-dibromopropane that was used was enriched to the extent of 2.0 mCi/mol.

3-Phenoxy[2-^{14}C]propyl bromide was prepared in 59% yield by the method of Marvel and Tanenbaum.[14] The product was purified by

(10) Bell, R. P. *The Tunnel Effect in Chemistry*; Chapman and Hall: New York, 1980; pp 60–63.

(11) Swartz, G. L.; Gulick, W. M. *J. Labelled Compd.* **1975**, *11*, 525.
(12) Shine, H. J.; Habdas, J.; Kwart, H.; Brechbiel, M.; Horgan, A. G.; San Filippo, J., Jr. *J. Am. Chem. Soc.* **1983**, *105*, 2823. Rhee, E. S.; Shine, H. J. *J. Org. Chem.* **1987**, *52*, 5633.
(13) Bak, B.; Led, J. J. *J. Labelled Compd.* **1968**, *4*, 22. Ott, D. G. *Synthesis with Stable Isotopes*; Wiley: New York, 1981; p 128.
(14) Marvel, C. S.; Tanenbaum, A. L. *J. Am. Chem. Soc.* **1922**, *44*, 2645. *Organic Syntheses*; Wiley: New York, 1941; Collect. Vol. I, pp 435–436.

chromatography on a column of silica gel with petroleum ether elution. A solution of 3-phenoxy[2-¹⁴C]propyl bromide (4.1 g, 0.019 mol) in 10 mL of a 33% solution of trimethylamine in ethanol was allowed to stand at room temperature. The product, *N,N,N*-trimethyl-*N*-(3-phenoxy[2-¹⁴C]propyl)ammonium bromide, began to precipitate within 1 h. After 24 h, 5.1 g (0.019 mol, 100%) of product was removed, allowed to dry in the air, and converted in 65% yield into [β-¹⁴C]allyl phenyl ether by treatment with freshly prepared silver oxide, as described earlier.[15]

Rearrangements and Isotope Measurements. Rearrangement of allyl phenyl ether was carried out at 220 °C. The product, *o*-allylphenol, was isolated and converted into the phenylurethane, which was purified with sublimation for scintillation counting. The details have been given earlier.[3] A sample of the phenylurethane was weighed on a Cahn balance

and was dissolved in 10 mL of cocktail (Fischer Biotech ScintiLene BD, No. BP 455-4). The sample was counted 30 times, that is, three times per cycle for 10 cycles. The 2σ was set at 0.5%. Four samples (replicates) from each conversion were weighed, so that each ¹⁴C count was eventually from an average of four samples counted as described. Three low conversions and one complete conversion constituted each rearrangement, and two rearrangements were performed. KIE are calculated as described earlier and are listed in Table I.

(15) Kupczyk-Subotkowska, L.; Shine, H. J. *J. Labelled Compd. Radiopharm.* **1986**, *24*, 303.

Nature of the Reactive Intermediates from the Iron-Induced Activation of Hydrogen Peroxide: Agents for the Ketonization of Methylenic Carbons, the Monooxygenation of Hydrocarbons, and the Dioxygenation of Arylolefins

Hui-Chan Tung, Chan Kang, and Donald T. Sawyer*

Contribution from the Department of Chemistry, Texas A&M University, College Station, Texas 77843. Received November 6, 1991

Abstract: The reaction efficiencies and product selectivities for a group of ML/HOOH/substrate/solvent systems have been evaluated. The catalysts include Fe^{II}(PA)$_2$, Fe^{II}(DPA)$_2^{2-}$, Fe^{III}Cl$_3$, [Fe^{II}(OPPh$_3$)$_4$](ClO$_4$)$_2$, [Fe^{II}(bpy)$_2$](ClO$_4$)$_2$, [Fe^{II}(MeCN)$_4$](ClO$_4$)$_2$, [Fe^{II}(O$_2$bpy)$_2$](ClO$_4$)$_2$, and [Co^{II}(bpy)$_2$](ClO$_4$)$_2$, the solvents include (py)$_2$HOAc, (MeCN)$_4$py, and MeCN, and the substrates include c-C$_6$H$_{12}$, PhCH$_3$, PhCH$_2$CH$_3$, c-C$_6$H$_{10}$, and c-PhCH=CHPh. When the HOOH/ML ratio is at least 10, all of the complexes catalytically ketonize methylenic carbons and dioxygenate arylolefins. The most effective catalyst systems are Fe^{II}(PA)$_2$/py$_2$(HOAc) (e.g., with c-C$_6$H$_{12}$ the process is 70% efficient and 95% selective), Fe^{II}(OPPh$_3$)$_4^{2+}$/MeCN, and Co^{II}(bpy)$_2^{2+}$/(MeCN)$_4$py, which activate nucleophilic HOOH via their electrophilicity. The reactive intermediates appear to be [(PA)$_2$Fe^{IV}(OH)(OOH), 3], [(Ph$_3$PO)$_4^{2+}$Fe^{IV}(OH)(OOH), 3'], and [(bpy)$_2^{2+}$Co^{IV}(OH)(OOH), 3'''], which are representative of all of the catalysts. These same intermediates also dioxygenate arylolefins. A precursor intermediate [a one-to-one ML/HOOH adduct; e.g., [(PA)$_2^-$Fe^{II}OOH + pyH$^+$, 1]] monooxygenates (oxidizes) hydrocarbons to alcohols and Rpy and reacts with excess HOOH to form species 3. Although the latter is the favored path for the Fe^{II}(PA)$_2$/(py)$_2$HOAc and Co^{II}(bpy)$_2^{2+}$/(MeCN)$_4$py systems, the monooxygenation path is dominant for the Fe^{III}Cl$_3$/MeCN and Fe^{II}(OPPh$_3$)$_4^{2+}$/MeCN systems. In the presence of olefins, species 1 undergoes dehydration to (PA)$_2$Fe^{IV}=O, 2, which transforms them to epoxides. Similar intermediates and reaction paths are observed when *t*-BuOOH is used in place of HOOH. With *t*-BuOOH the reactivity of species 1 with substrate (RH) becomes dominant to give Rpy or ROH, and species 3 reacts with methylenic carbons to give mixtures of ROOBu-*t* and ketone. Evaluation of the kinetic isotope effect with cyclohexane and toluene for the full range of catalysts and solvents gives k_H/k_D values of 2.4 to >10 for the ketonization of c-C$_6$H$_{12}$, 2.7-4.7 for PhCH$_3$, 1.4-2.9 for the hydroxylation process, and 1.7 for the Rpy production process [Fe^{II}(PA)$_2$/(py)$_2$HOAc/c-C$_6$H$_{12}$].

During the past decade, several reports have discussed the iron-induced activation of hydrogen peroxide (HOOH) for the catalytic and selective oxygenation of hydrocarbon substrates via non-Fenton-chemistry pathways. The transformations have included the following: (a) the ketonization of methylenic carbons [e.g., c-C$_6$H$_{12}$ → c-C$_6$H$_{10}$(O)] with (i) a Fe^{III}Cl$_3$/HOOH/(py)$_4$HOAc system,[1] (ii) a Fe^{II}(PA)$_2$/HOOH/(py)$_2$HOAc system (PA, anion of picolinic acid),[2] and (iii) a Co^{II}(bpy)$_2^{2+}$/HOOH/(MeCN)$_4$py system;[3] (b) the dioxygenation of arylolefins and acetylenes with (i) a Fe^{II}(MeCN)$_4^{2+}$/HOOH/MeCN system,[4,5] (ii) a Fe^{III}Cl$_3$/HOOH/MeCN system,[6] (iii) a Fe^{II}(PA)$_2$/HOOH/(py)$_2$HOAc system,[2] and (iv) a Co^{II}(bpy)$_2^{2+}$/

HOOH/(MeCN)$_4$py system;[3] and (c) the epoxidation of olefins with the preceding four systems.[2-6] Although there is good evidence that the reactive intermediate for olefin epoxidation is a ferryl (L$_x$Fe^{IV}=O) or perferryl (L$_y$Fe^V=O) species,[7] there is complete discord as to the formulation(s) of the activated complex for the (a) ketonization and (b) dioxygenation processes. The latest propositions[8,9] of the Barton group envision the interaction of a binuclear (μ-oxo)[iron(III)] complex with HOOH to give [L$_n$Fe^{III}OFe^V(O)L$_n$], which selectively reacts with R$_2$CH$_2$ to form an iron-carbon σ-bond (intermediate A). The latter is believed to react with a second HOOH to form an intermediate [L$_n$Fe^{III}OFe^V(OOH)(CHR$_2$)] that collapses to give R$_2$CH(OOH) and ketone. They also suggest that some of intermediate A re-

(1) Barton, D. H. R.; Halley, F.; Ozbalik, N.; Young, E. *New J. Chem.* **1989**, *13*, 177.
(2) Sheu, C.; Richert, S. A.; Cofré, P.; Ross, B., Jr.; Sobkowiak, A.; Sawyer, D. T.; Kanofsky, J. R. *J. Am. Chem. Soc.* **1990**, *112*, 1936-1942.
(3) Tung, H.-C.; Sawyer, D. T. *J. Am. Chem. Soc.* **1990**, *112*, 8214-8215.
(4) Sugimoto, H.; Sawyer, D. T. *J. Am. Chem. Soc.* **1984**, *106*, 4283-4285.
(5) Sugimoto, H.; Sawyer, D. T. *J. Am. Chem. Soc.* **1985**, *107*, 5712-5716.
(6) Sugimoto, H.; Sawyer, D. T. *J. Org. Chem.* **1985**, *50*, 1784-1786.

(7) Sugimoto, H.; Tung, H.-C.; Sawyer, D. T. *J. Am. Chem. Soc.* **1988**, *110*, 2465.
(8) Barton, D. H. R.; Doller, D.; Balavoine, G. *J. Chem. Soc., Chem. Commun.* **1990**, 1787.
(9) Barton, D. H. R.; Doller, D.; Ozbalik, N.; Balavoine, G. *Proc. Natl. Acad. Sci. U.S.A.* **1990**, *87*, 3401.